Electron impact excitation rate coefficients of N II ion*

Yang Ning-Xuan(杨宁选)[a], Dong Chen-Zhong(董晨钟)[a)b)†],
Jiang Jun(蒋 军)[a], and Xie Lu-You(颉录有)[a]

[a] College of Physics and Electronics Engineering, Northwest Normal University, Lanzhou 730070, China
[b] Joint Laboratory of Atomic and Molecular Physics, NWNU&IMP CAS, Lanzhou 730070, China

(Received 6 May 2009; revised manuscript received 23 February 2010)

This paper calculates the electron impact excitation rate coefficients from the ground term $2s^22p^2\ ^3P$ to the excited terms of the $2s^22p^2$, $2s2p^3$, $2s^22p3s$, $2s^22p3p$, and $2s^22p3d$ configurations of N II. In the calculations, multiconfiguration Dirac–Fork wave functions have been applied to describe the target-ion states and relativistic distorted-wave calculation has been performed to generate fine-structure collision strengths. The collision strengths are then averaged over a Maxwellian distribution of electron velocities in order to generate the effective collision strengths. The calculated rate coefficients are compared with available experimental and theoretical data, and some good agreements are found for the outer shell electron excitations. But for the inner shell electron excitations there are still some differences between the present calculations and available experiments.

Keywords: relativistic distorted-wave method, multiconfiguration Dirac–Fork method, configuration interaction, rate coefficients

PACC: 3120, 3130, 3450H, 3480D

1. Introduction

Nitrogen is amongst the most abundant chemical elements and is essential to life on earth. The intensities of emission lines from N II have been used for temperature and density diagnostics of low density astrophysical plasmas.[1−4] For example, in the optical spectrum, the line intensity ratios I(575.62)/[I(654.99)+I(658.52)], where the 575.62 nm, 654.99 nm and 658.52 nm arise from the transitions $2s^22p^2\ ^1D_2$ - $2s^22p^2\ ^1S_0$, $2s^22p^2\ ^3P_1$ - $2s^22p^2\ ^1D_2$ and $2s^22p^2\ ^3P_2$ - $2s^22p^2\ ^1D_2$ respectively, have been used for electron temperature diagnostic.[2] In the infrared spectrum, Keenan *et al.* have carried out an electron density diagnostic based on the $2s^22p^2\ ^3P_1$ - $2s^22p^2\ ^3P_2$ and $2s^22p^2\ ^3P_0$ - $2s^22p^2\ ^3P_1$ transitions.[3] In the ultraviolet region lines at 213.97 nm and 214.35 nm, arising from the $2s^22p^2\ ^3P_1$ - $2s2p^3\ ^5S_2$ and $2s^22p^2\ ^3P_2$ - $2s2p^3\ ^5S_2$ transitions, have been used in conjunction with the 654.99 nm and 658.52 nm optical lines to provide information about the coronal plasma.[4]

In theory, the diagnostic line intensity ratios can be calculated by using electron impact excitation rates in low density plasmas where collisional coupling and radiative cascades can be neglected. In the 1970s, Saraph *et al.*,[5,6] Smith *et al.*,[7] Henry *et al.*[8] and Ormonde *et al.*[9] calculated electron impact excitation strengths for transitions among the ground configuration terms of N II by using close-coupling expansion methods. In the 1990s, Lennon and Burke[10] and Stafford *et al.*[11] calculated the effective collision strengths from the ground term to the all excited terms of the $2s^22p^2$, $2s2p^3$, $2s^22p3s$, and $2s^22p3p$ configurations of N II by using 12-state and 13-state R-matrix method. However, significant differences have been found in the effective collision strengths between the 12-state and 13-state R-matrix calculations. Particularly at low temperatures, the results of the 12-state and 13-state R-matrix are found to differ by up to a factor of two. In 1998, Frost *et al.*[12] measured the rate coefficients from the ground term $2s^22p^2\ ^3P$ to all the terms of the $2s2p^3$, $2s^22p3s$, $2s^22p3p$ and $2s^22p3d$ configurations of N II. They also calculated the rate coefficients by using R-matrix method. The discrepancy between experiment and theory is 50 percent for some transitions. In order to interpret these discrepancies, 23-state R-matrix calculation was carried out by Husdson and Bell in 2005.[1] It was found that the results of effective collision strengths agreed with those of Lennon and Burke[10] within 10 percent, but disagreed with the calculations of Stafford *et al.*[11] Furthermore, their rate coefficients are also in good

*Project supported by the National Natural Science Foundation of China (Grant Nos. 10774122 and 10876028), the Specialized Research Fund for the Doctoral Program of Higher Education of China (Grant No. 20070736001), and the Technology and Innovation Program of Northwest Normal University (Grant No. NWNU-KJCXGC-03-21).

†Corresponding author. E-mail: dongcz@nwnu.edu.cn

© 2010 Chinese Physical Society and IOP Publishing Ltd

agreement with the calculations of Frost *et al.*,[12] but differences with their measurement[12] are large, especially for the $2s^22p^2\ ^3P$ - $2s^22p3d\ ^3D$ and $2s^22p^2\ ^3P$ - $2s^22p3d\ ^3P$ transitions.

In this paper, we calculate the excitation rate coefficients from the ground term $2s^22p^2\ ^3P$ to the all excited terms of the $2s^22p^2$, $2s2p^3$, $2s^22p3s$, $2s^22p3p$, and $2s^22p3d$ configurations of N II by using relativistic distorted-wave (RDW) method. We also compare our calculations with the available experimental and theoretical results for the transitions from the ground term to the $2s^22p3s\ ^1P$, $2s2p^3\ ^1D$, $2s^22p3p\ ^3S$, $2s2p^3\ ^3S$, $2s^22p3d\ ^3P$, and $2s^22p3d\ ^3D$ terms. A better agreement between the present calculations and the experiments of Frost *et al.*[12] has been found.

2. Theoretical method

The RDW method is used to calculate the collision strengths for electron impact excitation, as described by Pindzola and Arter,[13] Hagelstein,[14,15] Zhang and Sampson,[16−18] Chen,[19] Zemana *et al.*[20] and so on. Recently, a new full RDW programme has been developed by us.[21−24] So only a brief description of the method is given here. The wavefunctions of the target states are generated by the widely used atomic structure package Grasp92[25] based on the multiconfiguration Dirac–Fock method. The wavefunctions for both the initial and final states of the impact systems are the antisymmetric wavefunctions of the total $(N+1)$-electron system including the target ion plus a continuum electron, which can be written as[21−24]

$$\Psi = \frac{1}{(N+1)^{1/2}} \sum_{p=1}^{N+1} (-1)^{N+1-p} \times \sum_{M_t,\, m} C(J_t j M_t m; JM) \Phi_{\beta_t J_t}(x_p^{-1}) u_{\kappa m \varepsilon}(x_p), \quad (1)$$

where C is Clebsch–Gordon coefficient, J_t, j, and J are the angular momentum quantum numbers of the target ion, continuum electron and the impact system, respectively, $\Phi_{\beta_t J_t}$ are the target-ion wave functions, β_t represents all other quantum numbers in addition to J_t, x_p designates the space and spin coordinates for electron p and x_p^{-1} is the space and spin coordinates of all the N electrons other than p, $u_{\kappa m \varepsilon}$ is the RDW Dirac spinor for a continuum electron, and κ is the relativistic quantum number. The continuum orbitals with given electron energy are solutions of the Coupled-Dirac equations[21−24,26,27] in which the direct and exchange potentials are considered in the total $(N+1)$-electron system.

The RDW electron impact excitation (EIE) collision strength Ω_{if} from an initial state i to final state f can be written as[21,23,24,26]

$$\Omega_{if}(\varepsilon) = 8 \sum_J (2J+1) \sum_{\kappa,\, \kappa'} |\langle \Psi_{\rm i}| \sum_{p,q\ p<q}^{N+1} (V_{\rm Coul} + V_{\rm Breit}) |\Psi_f\rangle|^2, \quad (2)$$

where κ and κ' are the relativistic quantum number of the initial and final continuum electrons, respectively, In the calculations of the EIE strengths, to ensure the convergence of the collision strengths, we have included explicitly all the partial waves up to $|\kappa| = 45$. The $V_{\rm Coul}$ is the Coulomb operator and $V_{\rm Breit}$ is the Breit operator.[28]

The collision strengths are averaged over a Maxwellian distribution of electron velocities to obtain the effective collision strength. For excitation from initial level i to final level f, the effective collision strength Υ_{if} at electron temperature $T_{\rm e}$ (in Kelvin) is given by[29]

$$\Upsilon_{if} = \int_0^\infty \Omega_{if} \exp\left(\frac{-\epsilon_{\rm i}}{kT_{\rm e}}\right) {\rm d}\left(\frac{\epsilon_{\rm i}}{kT_{\rm e}}\right), \quad (3)$$

where $\epsilon_{\rm i}$ is the energy of the incident electron and k is Boltzmann's constant.

Once the effective collision strength is determined, the excitation rate coefficient at electron temperature $T_{\rm e}$ (in Kelvin) is given as[29]

$$C_{if} = \frac{2\sqrt{\pi}\alpha c a_0^2}{g_{\rm i}} \sqrt{\frac{I_{\rm H}}{kT_{\rm e}}} \exp\left(\frac{\Delta E_{if}}{kT_{\rm e}}\right) \Upsilon_{if}, \quad (4)$$

where $g_{\rm i}$ is the statistical weight of the initial state, $I_{\rm H}$ is the ionization potential energy of hydrogen, $T_{\rm e}$ is the electron temperature and ΔE_{if} is the transition energy.

3. Results and discussions

In order to consider the correlation effects, in our calculations, three correlation models have been used to describe the target states. Model A includes the $2s^22p^2$, $2s2p^3$ and $2s^22p3l$ (l = 0, 1, 2) configurations, which generate 41 levels. Model B includes the $2s^22p^2$, $2s2p^3$, $2s^22p3l$ and $2s^22p4l$ (l = 0, 1, 2, 3) configurations, generating 79 levels. Model C includes

all the states in Model B and all the states from the $2s^22p5l$ (l = 0, 1, 2) configurations, in this case we have 105 levels. In Table 1 we list the calculated energy levels in Model A, B and C for the $2s^22p^2$, $2s2p^3$, $2s^22p3s$, $2s^22p3p$ and $2s^22p3d$ configurations, relative to the ground term $2s^22p^2\ ^3P$. These values are compared with the NIST values[30] and other theoretical results.[1,11,12] From the table, we can find that the results in Models A and B show some large discrepancies with the NIST values, therefore they can only provide a primary estimate for the target states, while the agreement between the current results in Model C and the values in NIST values is very good, and the differences are smaller than 1% in most cases. Clearly that the Model C is a good description for the target states.

Table 1. Comparison of energy levels (in Ry) for N II.

level	model A	model B	model C	NIST[30]	Hudson[1]	Frost[12]	Stafford[11]
$2s^22p^2\ ^3P$	0.0000	0.0000	0.0000	0.0000	0.0000	0.0008	0.0000
$2s^22p^2\ ^1D$	0.1411	0.1410	0.1408	0.1396	0.1485	0.1385	0.1548
$2s^22p^2\ ^1S$	0.2945	0.2943	0.2941	0.2979	0.3155	0.2964	0.3180
$2s2p^3\ ^5S$	0.4568	0.4457	0.4413	0.4263	0.4114	0.4245	0.4090
$2s2p^3\ ^3D$	0.8434	0.8412	0.8391	0.8406	0.8454	0.8377	0.8608
$2s2p^3\ ^3P$	0.9986	0.9915	0.9914	0.9953	1.0108	0.9921	1.0366
$2s2p^3\ ^1D$	1.3866	1.3576	1.3391	1.3139	1.3350	1.3099	1.3528
$2s^22p3s\ ^3P$	1.3948	1.3822	1.3691	1.3579	1.3560	1.3538	1.4060
$2s^22p3s\ ^1P$	1.3997	1.3891	1.3799	1.3595	1.3615	1.3554	1.4126
$2s2p^3\ ^3S$	1.4850	1.4517	1.4153	1.4136	1.4389	1.4093	1.4502
$2s^22p3p\ ^1P$	1.5480	1.5295	1.5173	1.5000	1.5240	1.4955	1.5258
$2s^22p3p\ ^3D$	1.5628	1.5437	1.5220	1.5183	1.5413	1.5138	1.5382
$2s2p^3\ ^1P$	1.5741	1.5526	1.5241	1.5197	1.5605	1.5152	1.5982
$2s^22p3p\ ^3S$	1.5857	1.5730	1.5568	1.5391	1.5587	1.5345	
$2s^22p3p\ ^3P$	1.6186	1.5823	1.5760	1.5550	1.5690	1.5503	
$2s^22p3p\ ^1D$	1.6471	1.5973	1.5883	1.5875	1.5987	1.5828	
$2s^22p3p\ ^1S$	1.7077	1.6711	1.6496	1.6245	1.6315	1.6197	
$2s^22p3d\ ^3F$	1.7501	1.7359	1.7084	1.7003	1.7006	1.6953	
$2s^22p3d\ ^1D$	1.7621	1.7418	1.7112	1.7049	1.7056	1.6999	
$2s^22p3d\ ^3D$	1.7658	1.7496	1.7150	1.7084	1.7085	1.7034	
$2s^22p3d\ ^3P$	1.7781	1.7587	1.7378	1.7212	1.7218	1.7162	
$2s^22p3d\ ^1F$	1.7943	1.7623	1.7385	1.7253	1.7279	1.7203	
$2s^22p3d\ ^1P$	1.8147	1.7765	1.7390	1.7325	1.7366	1.7274	

In order to compare with the experimental and other theoretically term-dependent results. The present calculated collision strengths are combined by weighted average on the level to level collision strengths,

$$\Omega(I,F) = \frac{\sum_{if}(2J_{\rm i}+1)\Omega_{if}(\varepsilon)}{\sum_{i}(2J_{\rm i}+1)}, \qquad (5)$$

where I and F represent the initial and final target terms respectively, i and f are the corresponding fine-structure levels. Rate coefficients were then created using these $\Omega(I,F)$ collision strengths by applying Eqs. (3) and (4).

In Fig. 1 the rate coefficients for the transitions from the ground term $2s^22p^2\ ^3P$ to the excited terms $2s2p^3\ ^1D$, $2s^22p3s\ ^1P$, $2s2p^3\ ^3S$, $2s^22p3p\ ^3S$, $2s^22p3d\ ^3D$ and $2s^22p3d\ ^3P$ are shown in the three correlation models, and compared with the experiments of Frost *et al.*[12] and the calculations of Frost *et al.*,[12] Hudson and Bell[1] and Stafford *et al.*[11] For easiness of comparison, the data obtained from the current calculations are displayed using the same scales as the figures presented in Frost *et al.*[12]- covering an electron temperature range of 2–12 eV. Figures 1(a) and 1(b) exhibit the rate coefficients for the 2p → 3d outer shell electron excitations, namely from $2s^22p^2\ ^3P$ to $2s^22p3d\ ^3P$ and $2s^22p3d\ ^3D$ transitions. As can be seen from the figure, the results in Models A and B are higher than those in the Model C, the distinction amongst them is also big. The results of the Model

A are more close to the results of Hudson *et al.* using 23-state R-matrix.[1] And the calculations of Hudson and Bell[1] agree with the R-matrix calculation of Frost *et al.*[12] But for these two transitions, the measured rates are about a factor of 10 less than their data. However, our results in Model C are in better agreement with the measured rate coefficients of Frost *et al.*[12] than those calculated by Hudson and Bell[1] and Frost *et al.*[12] These show that the correlation effects for 2p → 3d valence-electron excitations are crucial. In Figs. 1(c) and 1(d), the rate coefficients for the 2p → 3s and 2p → 3p valence-electron excitations of namely the $2s^22p^2\ ^3P$ - $2s^22p3s\ ^1P$ and $2s^22p^2\ ^3P$ - $2s^22p3p\ ^3S$ excitations are displayed. It can be seen that the difference of the current calculations in Models A, B and C for these two excitations are very small, all of the theoretical results, including the results of Hudson and Bell[1] and Frost *et al.*,[12] agree with the measured rate coefficients values of Frost *et al.*[12] excellently. So, the correlation effects for 2p → 3s and 2p → 3p excitations are inconspicuous. Figures 1(e) and 1(f) show the rate coefficients for the 2s → 2p of inner shell electrons $\Delta n = 0$ excitations, namely the $2s^22p^2\ ^3P$ - $2s2p^3\ ^1D$ and $2s^22p^2\ ^3P$ - $2s2p^3\ ^3S$ excitations. We found that the results of R-matrix lie closer to the measured values of Frost *et al.*[12] for the rate coefficients of the $2s^22p^2\ ^3P$ - $2s2p^3\ ^1D$ transition. But the current RDW calculated data are lower than the measured results of Frost *et al.*[12] For the rate coefficients of the $2s^22p^2\ ^3P$ - $2s2p^3\ ^3S$ transition, we found that the calculations of Stafford *et al.*,[11] Frost *et al.*[12] and Hudson and Bell[1] by using R-matrix are larger than the measured values of Frost *et al.*,[12] but present results in RDW are smaller than the experimental values.[12] So for the 2s → 2p electron excitation of inner shell $\Delta n = 0$, the further studies of theory and experiment are needed.

Based on above discussions, we also calculate the rate coefficients from ground state $2s^22p^2\ ^3P$ to $2s2p^3\ ^3D$, ^3P, ^1D, ^1P, ^3S and $2s^22p3s\ ^3P$, ^1P and $2s^22p3p\ ^3P$, ^1P, ^3S, ^1S and $2s^22p3d\ ^1D$, ^3D, ^1P, ^3P, ^3F, ^1F transitions in Models A, B and C. These transitions have also been observed by Frost *et al.*[12] using spectroscope. For the numerical simulations of level population and spectrum, the rate coefficients of these transitions are needed. Frost *et al.*[12] measured part of data, but they do not give their results in digital form. In Table 2, the values of these excitations are given.

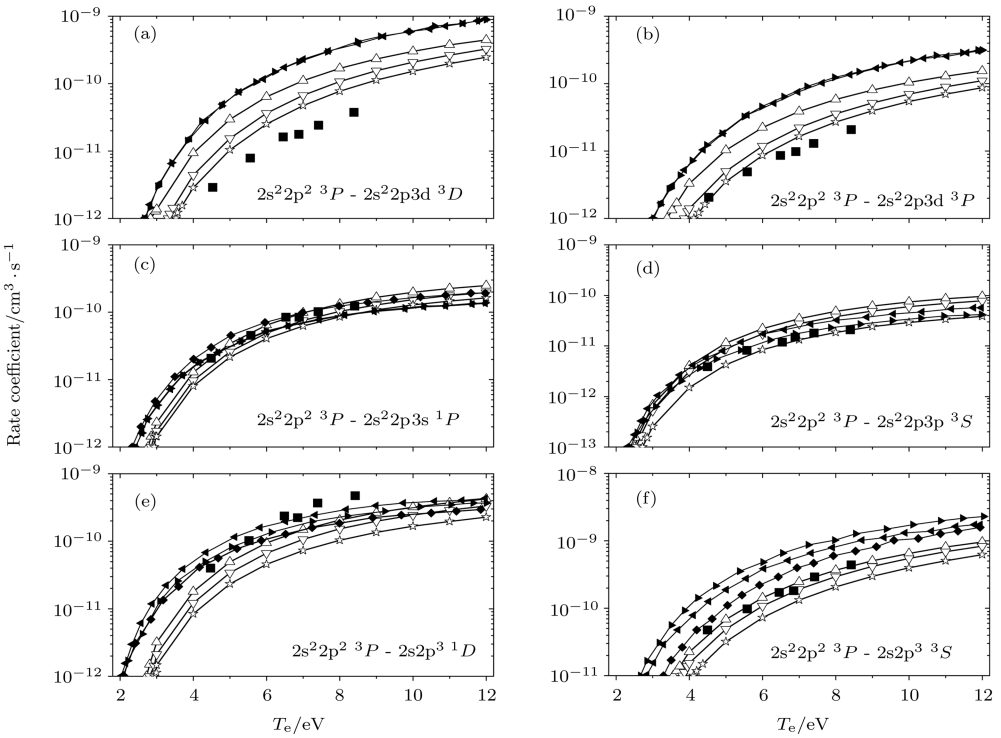


Fig. 1. Rate coefficients of N II from the $2s^22p^2\ ^3P$ to the $2s2p^3\ ^1D$, $2s^22p3s\ ^1P$, $2s2p^3\ ^3S$, $2s^22p3p\ ^3S$, $2s^22p3d\ ^3D$ and $2s^22p3d\ ^3P$. The up-triangles are the results in model A, the down-triangles are the results in model B, the pentagons are the results in model C. The squares are the experiments of Frost *et al.*,[12] the left-triangles are the R-matrix results of Frost *et al.*,[12] the right-triangles are the 23-state R-matrix results of Hudson and Bell,[1] the rhombuses are the 13-state R-matrix results of Stafford *et al.*[11]

Table 2. Calculated rate coefficients (in $\mathrm{cm}^3 \cdot \mathrm{s}^{-1}$) for electron impact excitation of N II from ground state $2s^2 2p^2\ ^3P$. In each case upper, middle and lower entries are calculated in models A, B and C, respectively.

		T_e/eV				
configuration	term	3.0	5.0	8.0	10.0	12.0
		1.968×10^{-10}	1.037×10^{-09}	2.646×10^{-09}	3.613×10^{-09}	4.441×10^{-09}
	^3D	1.268×10^{-10}	7.505×10^{-10}	2.115×10^{-09}	3.000×10^{-09}	3.787×10^{-09}
		8.833×10^{-11}	4.819×10^{-10}	1.295×10^{-09}	1.818×10^{-09}	2.286×10^{-09}
		4.840×10^{-11}	3.447×10^{-10}	1.086×10^{-09}	1.604×10^{-09}	2.082×10^{-09}
	^3P	3.661×10^{-11}	2.903×10^{-10}	9.748×10^{-10}	1.470×10^{-09}	1.935×10^{-09}
$2s2p^3$		2.871×10^{-11}	2.045×10^{-10}	6.585×10^{-10}	9.902×10^{-10}	1.309×10^{-09}
		3.186×10^{-12}	4.911×10^{-11}	2.055×10^{-10}	3.203×10^{-10}	4.229×10^{-10}
	^1D	2.115×10^{-12}	3.402×10^{-11}	1.516×10^{-10}	2.446×10^{-10}	3.323×10^{-10}
		1.459×10^{-12}	2.333×10^{-11}	1.033×10^{-10}	1.666×10^{-10}	2.269×10^{-10}
		8.897×10^{-13}	1.607×10^{-11}	7.694×10^{-11}	1.268×10^{-10}	1.743×10^{-10}
	^1P	3.778×10^{-13}	7.938×10^{-12}	4.498×10^{-11}	7.999×10^{-11}	1.164×10^{-10}
		1.983×10^{-13}	4.068×10^{-12}	2.278×10^{-11}	4.058×10^{-11}	5.940×10^{-11}
		9.119×10^{-13}	1.429×10^{-11}	6.161×10^{-11}	9.840×10^{-11}	1.337×10^{-10}
	^3P	7.937×10^{-13}	1.263×10^{-11}	5.587×10^{-11}	9.055×10^{-11}	1.246×10^{-10}
$2s^22p3s$		6.463×10^{-13}	1.069×10^{-11}	5.005×10^{-11}	8.374×10^{-11}	1.183×10^{-10}
		2.307×10^{-12}	3.428×10^{-11}	1.330×10^{-10}	1.971×10^{-10}	2.486×10^{-10}
	^1P	1.732×10^{-12}	2.604×10^{-11}	1.028×10^{-10}	1.541×10^{-10}	1.964×10^{-10}
		1.431×10^{-12}	2.155×10^{-11}	8.546×10^{-11}	1.285×10^{-10}	1.643×10^{-10}
		1.088×10^{-12}	1.782×10^{-11}	7.555×10^{-11}	1.167×10^{-10}	1.521×10^{-10}
	^1P	8.916×10^{-13}	1.481×10^{-11}	6.413×10^{-11}	1.003×10^{-10}	1.322×10^{-10}
		6.190×10^{-13}	1.012×10^{-11}	4.299×10^{-11}	6.651×10^{-11}	8.684×10^{-11}
		6.846×10^{-13}	1.135×10^{-11}	4.810×10^{-11}	7.390×10^{-11}	9.569×10^{-11}
	^3S	5.246×10^{-13}	8.829×10^{-12}	3.822×10^{-11}	5.947×10^{-11}	7.786×10^{-11}
$2s^22p3p$		2.529×10^{-13}	4.276×10^{-12}	1.863×10^{-11}	2.911×10^{-11}	3.825×10^{-11}
		2.127×10^{-12}	3.925×10^{-11}	1.905×10^{-10}	3.165×10^{-10}	4.397×10^{-10}
	^3P	1.350×10^{-12}	2.633×10^{-11}	1.366×10^{-10}	2.347×10^{-10}	3.349×10^{-10}
		5.049×10^{-13}	1.069×10^{-11}	6.099×10^{-11}	1.101×10^{-10}	1.641×10^{-10}
		2.230×10^{-13}	4.073×10^{-12}	1.875×10^{-11}	2.990×10^{-11}	3.985×10^{-11}
	^1S	9.118×10^{-14}	1.751×10^{-12}	8.564×10^{-12}	1.409×10^{-11}	1.927×10^{-11}
		1.798×10^{-14}	3.753×10^{-13}	2.033×10^{-12}	3.519×10^{-12}	5.009×10^{-12}
		3.658×10^{-12}	6.644×10^{-11}	3.007×10^{-10}	4.745×10^{-10}	6.272×10^{-10}
	^3F	3.663×10^{-12}	6.664×10^{-11}	3.023×10^{-10}	4.777×10^{-10}	6.323×10^{-10}
		3.603×10^{-12}	6.436×10^{-11}	2.845×10^{-10}	4.435×10^{-10}	5.806×10^{-10}
		1.108×10^{-12}	2.003×10^{-11}	9.005×10^{-11}	1.413×10^{-10}	1.855×10^{-10}
	^1D	2.968×10^{-13}	6.145×10^{-12}	3.274×10^{-11}	5.614×10^{-11}	7.927×10^{-11}
		1.064×10^{-13}	2.320×10^{-12}	1.310×10^{-11}	2.314×10^{-11}	3.349×10^{-11}
		1.366×10^{-12}	2.959×10^{-11}	1.681×10^{-10}	3.016×10^{-10}	4.465×10^{-10}
	^3D	5.610×10^{-13}	1.540×10^{-11}	1.070×10^{-10}	2.080×10^{-10}	3.250×10^{-10}
$2s^22p3d$		3.441×10^{-13}	1.041×10^{-11}	7.698×10^{-11}	1.534×10^{-10}	2.448×10^{-10}
		4.826×10^{-13}	1.034×10^{-11}	5.825×10^{-11}	1.041×10^{-10}	1.537×10^{-10}
	^3P	1.740×10^{-13}	5.000×10^{-12}	3.560×10^{-11}	6.980×10^{-11}	1.100×10^{-10}
		1.112×10^{-13}	3.538×10^{-12}	2.690×10^{-11}	5.406×10^{-11}	8.679×10^{-11}
		1.306×10^{-12}	2.297×10^{-11}	1.008×10^{-10}	1.565×10^{-10}	2.037×10^{-10}
	^1F	2.659×10^{-13}	5.373×10^{-12}	2.810×10^{-11}	4.775×10^{-11}	6.687×10^{-11}
		6.581×10^{-14}	1.427×10^{-12}	8.044×10^{-12}	1.419×10^{-11}	2.050×10^{-11}
		3.215×10^{-13}	5.573×10^{-12}	2.453×10^{-11}	3.831×10^{-11}	5.021×10^{-11}
	^1P	6.901×10^{-14}	1.404×10^{-12}	7.612×10^{-12}	1.322×10^{-11}	1.883×10^{-11}
		2.033×10^{-14}	4.549×10^{-13}	2.660×10^{-12}	4.766×10^{-12}	6.960×10^{-12}

4. Conclusions

In summary, we have performed an RDW calculation to determine rate coefficients of N II in different correlation models. A comparison has been made of the results with the measured and calculated data for the $2s^22p^2\ ^3P$ to the $2s^22p3s\ ^1P$, $2s2p^3\ ^1D$, $2s^22p3p\ ^3S$, $2s2p^3\ ^3S$, $2s^22p3d\ ^3P$, and $2s^22p3d\ ^3D$ transitions. We find that for 2p → 3d valence-electron excitations, when we consider more correlative configuration, some good agreements are obtained with the measured values of Frost *et al.* For 2p → 3s and 2p → 3p excitations, all theoretical calculations including different models and methods are close to experimental values and the correlation effects are inconspicuous. However, for the 2s → 2p excitation, which are the inner shell $\Delta n = 0$ electron excitations, the quite large distinctions exist between theory and experiment, it needs to further study. Based on this models, we also provide a lot of data from the ground term $2s^22p^2\ ^3P$ to all the terms of $2s2p^3$, $2s^22p3s$, $2s^22p3p$ and $2s^22p3d$ configurations of N II.

References

[1] Hudson C E and Bell K L 2005 *Phys. Scr.* **71** 268
[2] Aller L H 1984 *Astrophy. and Space Science Library* **112** 360
[3] Keenan F P, Crawford F L, Feibelman W A and Aller L H 2001 *Astrophys. J. Suppl.* **132** 103
[4] Czyzak S J, Keyes C D and Aller L H 1986 *Astrophys. J. Suppl.* **61** 159
[5] Saraph H E, Seaton M J and Shemming J 1966 *Proc. Phys. Soc.* **89** 27
[6] Saraph H E and Seaton M J 1974 *J. Phys.* B **7** L63
[7] Smith K, Conneely M J and Morgan L A 1969 *Phys. Rev.* **177** 196
[8] Henry R J W, Burke P G and Sinfailam A L 1969 *Phys. Rev.* **178** 218
[9] Ormonde S, Smith K, Torres B W and Davies A R 1973 *Phys. Rev.* A **8** 262
[10] Lennon D J and Burke V M 1994 *Astron. Astrophys. Suppl.* **103** 273
[11] Stafford R P, Bell K L, Hibbert A and Wijesundera W P 1994 *Mon. Not. R. Astron. Soc.* **268** 816
[12] Frost R M, Awakowicz P, Summers H P and Badnell N R 1998 *J. Appl. Phys.* **84** 2989
[13] Pindzola M S and Arter S L 1980 *Phys. Rev.* A **22** 898
[14] Hagelstein P L 1986 *Phys. Rev.* A **34** 874
[15] Hagelstein P L 1986 *Phys. Rev.* A **34** 924
[16] Sampson D H and Zhang H L 1989 *Phys. Rev.* A **40** 604
[17] Zhang H L and Sampson D H 1990 *Phys. Rev.* A **42** 5378
[18] Zhang H L and Sampson D H 1993 *Phys. Rev.* A **47** 208
[19] Chen G X 1996 *Phys. Rev.* A **53** 3227
[20] Zemana V, McEachranb R P and Stauffer A D 1998 *Eur. Phys. J.* D **1** 117
[21] Jiang J, Dong C Z, Xie L Y, Wang J G, Yan J and Fritzche S 2007 *Chin. Phys. Lett.* **24** 691
[22] Jiang J, Dong C Z, Xie L Y and Wang J G 2008 *Phys. Rev.* A **78** 022709
[23] Yang N X, Dong C Z and Jiang J 2009 *Chin. Phys. Lett.* **26** 053401
[24] Yang N X, Dong C Z and Jiang J 2009 *Chin. Phys. Lett.* **26** 063401
[25] Parpia F A, Fischer C F and Grant I P 1996 *Comput. Phys. Commun.* **94** 247
[26] Jiang J, Dong C Z, Xie L Y, Zhou X X and Wang J G 2008 *J. Phys.* B **41** 24504
[27] Christopher J F, Sampson D H and Zhang H L 1993 *Phys. Rev.* A **47** 1009
[28] Dong C Z and Fritzche S 2005 *Phys. Rev.* A **72** 012507
[29] Kimura E, Nakazaki S, Eissner W B and Itikawa Y 1999 *Astron. Astrophys. Suppl.* **139** 167
[30] Ralchenko Y, Kramida A E and Reader J 2006 *NIST Atomic Spectra Database* http://physics. nist. gov/PhysRefData/ASD/index.html